Heliyon 9 (2023) e17168

Contents lists available at ScienceDirect

Heliyon

journal homepage: www.cell.com/heliyon

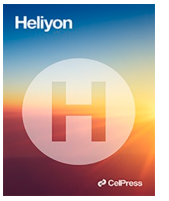

Ultrasonic-assisted extraction for phenolic compounds and antioxidant activity of Moroccan *Retama sphaerocarpa* L. leaves: Simultaneous optimization by response surface methodology and characterization by HPLC/ESI-MS analysis

Aafaf El Baakili [a], Mouhcine Fadil [a,b], Nour Eddine Es-Safi [a,*]

[a] *Mohammed V University in Rabat, LPCMIO, Materials Science Center (MSC), Ecole Normale Supérieure, Rabat, Morocco*
[b] *Laboratory of Applied Organic Chemistry, Sidi Mohamed Ben Abdellah University, P.O. Box 2202, Road of Imouzzer, Fez, Morocco*

ARTICLE INFO

Keywords:
Ultrasound-assisted extraction
Optimization
Response surface methodology
Retama sphaerocarpa
Phenolic compounds
Antioxidant activity

ABSTRACT

This study was designed to optimize the ultrasound-assisted extraction of phenolic compounds and the antioxidant activity of Moroccan *Retama sphaerocarpa* extracts using response surface methodology (RSM). A central composite design has been conducted to investigate the effects of three factors: extraction period (X_1), solvent concentration (X_2), and solvent-to-material ratio (X_3) on extraction yield, total phenolic content (TPC), flavonoids content (TFC), and antioxidant activity. The obtained results showed that the experimental values agreed with the predicted ones, confirming the capacity of the used model for optimizing the extraction conditions. The best extraction conditions for the simultaneous optimization were an extraction time of 38 min, a solvent concentration of 58%, and a solvent-to-material ratio of 30 mL/g. Under these conditions, the optimized values of yield, TPC, TFC, and DPPH-radical scavenging activity ($DPPH_{IC50}$) were 18.91%, 154.09 mg GAE/g, 23.76 mg QE/g, and 122.47 μg/mL, respectively. The further HPLC/ESI-MS analysis of the obtained optimized extract revealed the presence of 14 phenolic compounds with piscidic acid, vitexin, and quinic acid as major compounds. These research findings indicate promising applications for efficiently extracting polyphenolic antioxidants, especially in the food industry.

1. Introduction

Natural products discovery has recently gained considerable interest and has experienced a pronounced revival in the last two decades as the most successful class of drug leads [1]. They have received increasing attention especially with the worldwide pharmaceutical industry, with the growing population awareness and the high demand for herbal remedies promoting health advantages, cosmetics, and food processing industries [2]. Research on plant-based antioxidants is prompted by the fact that oxidative stress has a role in several illnesses [3].

Secondary metabolites which are often employed in medicines, nutraceuticals, food additives, and fine chemicals, are responsible for plants' therapeutic effects [4]. Among these phytochemicals, plants synthesize various different phenolic compounds with different physicochemical characteristics that are beneficial for human health [5].

* Corresponding author.
E-mail address: nour-eddine.es-safi@ens.um5.ac.ma (N.E. Es-Safi).

https://doi.org/10.1016/j.heliyon.2023.e17168
Received 22 March 2023; Received in revised form 7 June 2023; Accepted 8 June 2023
Available online 10 June 2023

Extraction constitutes a crucial step in recovering phytochemicals from plant matrix and biomass [6]. This facilitates the emergence of more effective and sustainable extraction techniques for plant phytochemicals [2]. Different extraction methods have been extensively used to extract plant-derived phenolic compounds, such as maceration, supercritical fluid extraction, percolation, microwave-assisted extraction, and Soxhlet extraction [7]. However, they are still negatively described as time-consuming, requiring large amounts of solvent, and giving low extraction yields [8]. Among the unconventional methods, ultrasound-assisted extraction (UAE) is an innovative technique that has recently earned greater attention as a low-cost, simple, and effective substitute of conventional extraction techniques to improve the extraction of bioactive compounds [9]. UAE offers improved reproducibility, easier manipulation, less solvent usage, and lower energy input than other procedures [10]. This method employs sound waves, which facilitate solvent penetration into the sample matrix by expanding the contact surface between the solid and liquid phases. As a result, the solutes quickly diffuse from the solid to the solvent, increasing the extract yields [11].

Performing extractions at low temperatures is another advantage of UAE. Indeed, this may reduce heat losses caused by high temperatures and prevent the degradation of biologically active substances due to side undesirable reactions such as hydrolysis, ionization, and/or oxidation [12], which makes them undesirable from an economic perspective [13]. Several bioactive components, including polysaccharides, flavonoids, anthocyanins, and phenolic compounds, have been effectively extracted using the UAE [14]. Compared to conventional techniques such as maceration or Soxhlet extraction, UAE generally gives higher antioxidant yields and markedly reduces extraction time [15].

Retama sphaerocarpa is the plant investigated in the present study. It's a perennial leguminous shrub with evergreen photosynthetic stems that belongs to the *Retama* genus. This plant grows in the Mediterranean region of North East Africa, the Iberian Peninsula, and North Africa [16]. *Retama* species may flourish in various soil types and climatic circumstances since they can withstand arid conditions [17]. This plant has been traditionally used to cure various illnesses, including diabetes, rheumatism, and inflammations [18]. Fresh fruits are thus typically used to cure diarrhea, while flowers infusions are generally used to treat liver problems [19]. The plant has been also applied as a purgative, anthelmintic, healing agent after circumcision, vulnerary, antibacterial, and sedative for the treatment of local wounds, skin ulcers, and wounds [20]. The pharmacological activities of *Retama* species has been widely studied, revealing antioxidant [21], antibacterial [22], hepatoprotective [23], anti-inflammatory [24], anti-proliferative [25], and antiviral activities [26]. These beneficial effects are obviously due to the presence of various phytochemicals such as alkaloids, fatty acids, phenolic acids, flavonoids, and other antioxidants known for their ability to lower the risk of degenerative diseases related to oxidative stress [27]. Given the importance of the extraction process as the first step for the separation and isolation of bioactive compounds, we were interested to explore the phytochemical extraction of *R. sphaerocarpa* leaves using UAE. In order to enhance the recovery of target compounds, the extraction parameters will be optimized. Although several phytochemicals in *Retama* extracts have been previously investigated, no research has been done to determine the best conditions for extracting bioactive compounds from the leaves of this species. Moreover, and to the best of our knowledge, no research has been done on recovering *R. sphaerocarpa*'s phytochemicals from Morocco. Therefore, this work aimed to find the best operating conditions for extracting bioactive products from the leaves of this species using the response surface methodology (RSM) technique and further determine its phenolic profile. The studied responses were the extraction yield, total phenolic and flavonoid contents and antioxidant activity. The extraction effectiveness is affected by several variables including solvent type and concentration, solid-solvent ratio, time, temperature, frequency of sonication and particle size [28]. Thus, the optimization of UAE allows the testing of several parameters likely to influence the extraction of phenolic compounds. Based on literature data, the most studied parameters in UAE optimization are the extraction time, the material-to-solvent ratio and the solvent concentration [28–34]. From this background, these three parameters were chosen to study their effect on the three responses yield, TPC, TFC and $DPPH_{IC50}$.

The present research reported thus for the first time an optimization study for the recovery of phenolic compounds from *R. sphaerocarpa* to obtain extracts with better antioxidant properties. The chosen central composite design (CCD) allowed us to investigate the impact of extraction parameters and their interaction on the studied responses, and then identify the best-operating conditions leading to their optimization.

2. Materials and methods

2.1. Plant material

Retama sphaerocarpa aerial parts were harvested in April 2020 from Ouaouizerth in the Middle-High Atlas near Azilal, Morocco. The plant identification was achieved at the laboratory of plant biology and physiology at the Scientific Institute in Rabat. The aerial plant parts were washed, dried to a constant weight for seven days at room temperature in the shade, grounded using an electric grinder (Taurus, Barcelona, Spain), and sieved to obtain a fine powder (particle size 500 μm). The powders were packed in a fresh-keeping polyethylene bags and stored in a refrigerator at 4 °C until needed.

2.2. Sample preparation

The extraction process was performed using an ultrasonic bath JEULIN no. 701 340 (bath power 220 V and continuous mode at 40 kHz). In a 100 mL capped brown flask, 5 g of *R. sphaerocarpa* powder was mixed with a specified amount of the extraction solution ethanol: water at a given concentration. The combination was maintained in a water bath at 50 °C at the same distance from the ultrasound sides under prescriptive ultrasonic power for a specific time according to the experiment design. This temperature (50 °C) was chosen after a preliminary test carried out by fixing all the parameters and varying only the temperature from 30 °C to 60 °C. The

suspensions were combined and filtered through Whatman's paper. The resulting filtrate was vacuum-vaporized at 40 °C on a rotary evaporator (Buchi R-210, Switzerland) and then refrigerated at 4 °C.

2.3. Determination of total phenolic content (TPC)

The Folin-Ciocalteu reagent was used to determine the total phenolic compounds concentration as described by Singleton et al. [35], with slight modifications. Briefly, 0.1 mL of each extract was combined with 0.1 mL of the Folin-Ciocalteu reagent for 5 min at room temperature. After neutralization with 10 mL of sodium carbonate solution 7.5%, the mixture was incubated for an additional hour. The absorbance was measures at 765 nm using a Lambda 25 Perkin-Elmer spectrophotometer (PerkinElmer, Waltham, MA, USA) having a wavelength range of 190–1100 nm and one fixed bandwidth equipped with 10 mm (path width) quartz cell. Gallic acid (0–0.225 g gallic acid/mL) was used as a standard to produce a linear calibration curve. The obtained results were expressed as mg gallic acid equivalents per gram of extract (mg GAE/g).

2.4. Determination of total flavonoid content (TFC)

Total flavonoid content was estimated by the colorimetric method using the aluminum chloride method previously reported by Lin et al., [36]. An aliquot of 500 μL of each extract was thoroughly mixed with 100 μL of 10% $AlCl_3$, 1.50 mL of 95% ethanol, 100 μL sodium acetate 1 M, and 2.80 mL distilled water. The absorbance was then determined at 415 nm. A quercetin standard calibration curve was used to carry out the quantification, and the findings were represented as mg of quercetin equivalents per gram of extract (mg QE/g).

2.5. DPPH free radical-scavenging activity

The capacity of *R. sphaerocarpa* to scavenge the DPPH radical was evaluated according to the method given by Pandey et al. [30]. Fifty μL of the explored samples at various concentrations were dissolved in methanol and then added to 2 mL of a 60 mM methanol solution of DPPH. The absorbance was recorded at 517 nm after 20 min at room temperature in the dark. Methanol with DPPH solution was used as a negative control, and the inhibition percentage of the DPPH free radical was calculated by using the following equation (Eq. (1)):

$$\%\ inhibition = \frac{(A_0 - A_1)}{A_0} \times 100 \quad (1)$$

A_0 stands for the sample used as a blank, and A_1 for the test sample's absorbance. By plotting the inhibition percentages against the sample concentrations, the sample concentration providing 50% inhibition (IC_{50}) was determined.

2.6. HPLC/ESI-MS analysis

The phenolic profile of the obtained extracts under optimized conditions has been explored with liquid chromatography coupled to a mass spectrometry detector. Analysis was performed on an Ultimate 3000 UHPLC apparatus consisting of a surveyor quaternary pump coupled to a PDA detector (200–600 nm), an electrospray ionization source, and an LCQ Advantage ion trap mass Thermo scientific spectrometer supplied by Orbitrap analyzer. A BDS Hypersil C18 column (150 mm × 4.6 mm × 5 μm) was used as a stationary phase. Water (A), acetonitrile (B), and acetonitrile (99:1, v/v), both containing 0.1% formic acid, formed the mobile phase at a flow rate of 0.48 mL/min. The used gradient was as follows: 0–5 min: 1% B, 5–8 min: 1–4.5% B, 8–20 min: 4.5–12% B, 20–22 min: 12–12.8% B, 22–27 min: 12.8–13.3% B, 27–33 min: 13.3–14.5% B, 33–48 min: 14.5–30% B, 48–55 min: 30–100% B, 55–59.5 min: 100–1% B then the column's re-equilibration for 5 min [27]. The column temperature was set at 45 °C, and the UV-visible detection range was set from 200 to 600 nm. UV spectra were also collected at 280 nm and 340 nm. Solutions with a concentration of 10 mg/mL were produced in MeOH: H_2O (50:50). A 0.2-m PTFE syringe filter was used to filter the resulting solution, and 20 L of the filtrate was then added to the HPLC apparatus. Phenolic compounds were identified based on UV and MS spectra in negative ion mode and by comparing the observed spectroscopic characteristics with those of literature data.

Table 1
Actual and coded levels of the independent variables used for the central composite design.

Independent variables	Coded variables	Variable levels			Unit
		−1	0	1	
Extraction time	X_1	20	40	60	Min
Solvent concentration	X_2	40	60	80	% (v/v)
Solvent-to-material ratio	X_3	10	20	30	mL/g

Table 2
Matrix of Central composite design with actual, predicted and residual results for Yield, Total phenol contents, Total flavonoids content and $DPPH_{IC50}$.

N° of experiments*	Factor's setting			Observed responses (**,***)											
	Time (min)	Solvent Concentration (% v/v)	Solvent to material Ratio (mL/g)	Yield (%)			TPC (mg GAE/g)			TFC (mg QE/g)			$DPPH_{IC50}$ (μg/mL)		
				Actual	Predicted	Residual	Actual	Predicted	Residual	Actual	Predicted	Residual	Actual	Predicted	Residual
1	20	40	10	15.05 ± 0.16^{c}	14.42	0.63	93.85 ± 0.23^{a}	88.38	5.47	23.28 ± 1.19^{cde}	23.07	0.21	197.20 ± 1.48^{i}	199.91	−2.71
2	60	40	10	25 ± 0.20^{fg}	24.23	0.77	123.2 ± 2.46^{de}	128.74	−5.54	25.03 ± 0.47^{ef}	22.62	2.41	134.5 ± 2.25^{c}	133.21	1.29
3	20	80	10	11.66 ± 0.91^{b}	11.59	0.07	110.45 ± 2.19^{c}	115.94	−5.49	34.3 ± 3.22^{ij}	32.24	2.06	188.85 ± 3.73^{h}	187.77	1.08
4	60	80	10	24.59 ± 1.39^{fg}	22.60	1.99	131.54 ± 0.64^{f}	131.07	0.47	30.5 ± 2.12^{gh}	32.97	−2.47	144.2 ± 4.27^{d}	145.30	−1.10
5	20	40	30	15.5 ± 2.62^{c}	17.13	−1.63	99.75 ± 2.40^{b}	100.11	−0.36	19.47 ± 1.26^{abc}	16.84	2.63	202.3 ± 2.83^{j}	204.38	−2.08
6	60	40	30	26.5 ± 0.45^{g}	26.20	0.30	144.02 ± 0.31^{h}	138.43	5.59	24.64 ± 0.20^{def}	26.54	−1.90	163.33 ± 2.36^{f}	167.60	−4.27
7	20	80	30	12.43 ± 1.12^{b}	12.83	−0.40	120.55 ± 4.89^{d}	114.91	5.64	31.86 ± 0.45^{hi}	34.12	−2.26	174.02 ± 4.24^{g}	178.49	−4.47
8	60	80	30	22.85 ± 0.23^{ef}	23.11	−0.26	122.63 ± 1.23^{de}	128.00	−5.37	44.94 ± 2.45^{k}	44.99	−0.05	165.47 ± 4.70^{f}	165.94	−0.47
9	20	60	20	14.40 ± 1.67^{bc}	17.86	−3.46	106.90 ± 3.20^{c}	101.81	5.09	22.15 ± 4.13^{bcde}	24.35	−2.20	160.05 ± 2.05^{ef}	158.61	1.44
10	60	60	20	21.46 ± 1.67^{de}	19.47	1.99	100.64 ± 2.49^{b}	106.14	−5.50	28.83 ± 2.38^{gh}	27.25	1.58	182.45 ± 2.35^{h}	171.16	11.29
11	40	40	20	25.55 ± 1.48^{g}	25.62	−0.07	124.95 ± 1.33^{de}	130.11	−5.16	16.45 ± 0.66^{a}	19.80	−3.35	163.00 ± 3.75^{f}	155.23	7.77
12	40	80	20	21.25 ± 0.35^{de}	22.65	−1.40	143.42 ± 3.25^{h}	138.68	4.74	36.35 ± 1.63^{j}	33.62	2.73	153.30 ± 1.17^{e}	148.33	4.97
13	40	60	10	10.10 ± 1.70^{a}	8.77	1.33	122.33 ± 1.53^{d}	127.60	−5.27	16.94 ± 1.30^{ab}	19.58	−2.64	171.66 ± 5.03^{g}	163.48	8.18
14	40	60	30	16.00 ± 0.17^{c}	18.81	−2.81	159.17 ± 4.34^{i}	154.32	4.85	26.81 ± 2.38^{fg}	24.79	2.02	128.41 ± 6.02^{a}	123.86	4.55
15	40	60	20	19.25 ± 1.47^{d}	18.79	0.46	136.29 ± 2.42^{g}	130.57	5.72	23.18 ± 2.86^{cde}	22.76	0.42	132.00 ± 0.7^{ab}	143.76	−11.76
16	40	60	20	19.30 ± 1.13^{d}	18.79	0.51	127.38 ± 2.47^{def}	130.57	−3.19	21.72 ± 0.83^{bcd}	22.76	−1.04	138.20 ± 5.23^{cd}	143.76	−5.56
17	40	60	20	20.75 ± 2.18^{de}	18.79	1.96	128.87 ± 3.89^{ef}	130.57	−1.70	24.64 ± 2.09^{def}	22.76	1.88	135.60 ± 0.85^{c}	143.76	−8.16

*Experiments were carried out after randomization.
**Each response is the average of three replicates with standard error.
***Means with different letters were significantly different at the level of $p < 0.05$.

Table 3
Variance analysis for the fitted models.

Source of variation	DF	Yield				TPC				TFC				$DPPH_{IC50}$			
		SS	MS	F	*p-value*	SS	MS	F	*p-value*	SS	MS	F	*p-value*	SS	MS	F	*p-value*
R	9	389.9	43.3	7.6	0.007*	4400.9	489.0	8.9	0.0044*	788.5	87.6	8.3	0.0054*	8085.0	898.3	10.6	0.0026*
r	7	39.8	5.7			385.3	55.1			73.7	10.5			591.9	84.6		
Lof	5	38.4	7.7	10.6	0.08	339.8	68.0	3.0	0.26	69.4	13.9	6.5	0.13	572.5	114.5	11.8	0.079
PE	2	1.5	0.7			45.6	22.8			4.3	2.1			19.4	9.7		
Total	16	429.7				4786.3					862.2			8676.9			
R^2		0.91				0.92				0.91				0.93			

DF: degrees of freedom; SS: sum of squares; MS: mean square; R: regression; r: residual; Lof: lack of fit; Pe: pure error; R^2: coefficient of determination; *: statistically significant.

2.7. Experimental design

The optimal combination of extraction factors for the phenolic compounds from *R. sphaerocarpa* was determined using a central composite design (CCD). Three levels (lower (1), middle (0), and upper (+1)) of a three-factor method were used in the tests. As independent variables that should be adjusted for the extraction, three primary parameters impacting extraction efficiency, namely, extraction time (min, X_1), ethanol concentration (%, X_2), and solvent-to-material ratio (mL/g, X_3), were selected. Their uncoded and coded values are shown in Table 1. The experimental domains of each factor were enlarged to cover more fluctuations of the responses, and then, to recognize a more diverse set of effects. A central composite design (CCD) with 17 runs in random order and three replicates in the central point was employed to forecast the parameters' linear, quadratic, and interaction effects. The chosen CCD consists of factorial points (experiments 1–8), axial points with $\alpha = 1$ (experiments 9–14), and center points (experiments 15–17).

2.7.1. Fitted model and statistical analysis

Multiple regression analysis was used to fit the data to the quadratic polynomial model shown in equation (Eq. (2)):

$$Y = b_0 + b_1X_1 + b_2X_2 + b_3X_3 + b_{12}X_1X_2 + b_{13}X_1X_3 + b_{23}X_2X_3 + b_{11}X_1^2 + b_{22}X_2^2 + b_{33}X_3^2 + \epsilon \quad (2)$$

where Y stands for the studied responses (extraction yield, total polyphenol content, flavonoid content, and DPPH free radical scavenging activity expressed by $DPPH_{IC50}$). b_0 represents the constant of the model, calculated as the average value of responses when all responses were at their level 0; b_1, b_2, and b_3 are coefficients of the main terms; b_{11}, b_{22}, and b_{33} are the coefficients of quadratic terms; b_{12}, b_{13}, and b_{23} are the coefficients of the interaction terms; X_1, X_2, and X_3 are the independent variables, while ε is the error term.

An analysis of variance (ANOVA) test at a 95% confidence level was performed to test the validity of the postulated model. Mean squares (MS) were obtained by dividing the sum of squares (SS) for each variation source (regression and residual) by the degree of freedom (DF). The F-value sufficiently describes the fluctuation of the data around its mean, and the model was statistically significant

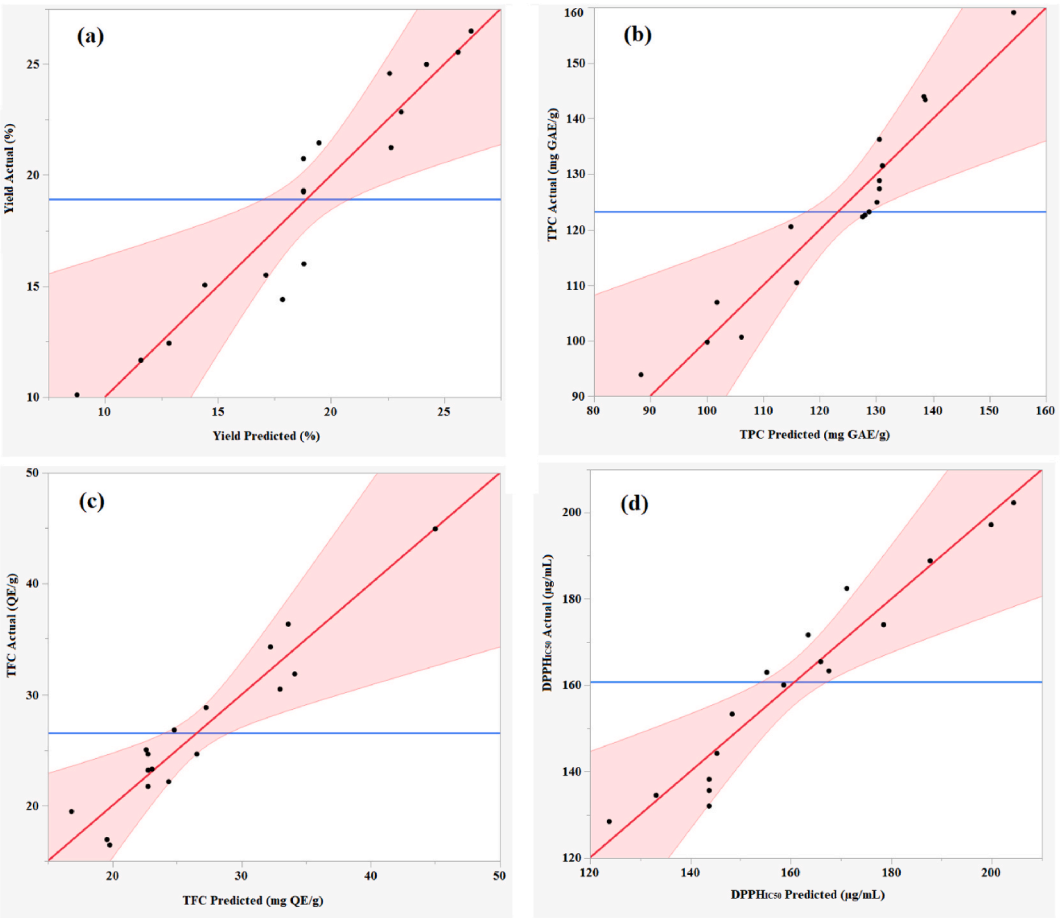

Fig. 1. The red lines represent the curve of actual values as a function of predicted ones for the four responses yield **(a)**, TPC **(b)**, TFC **(c)**, and $DPPH_{IC50}$ **(d)**. The horizontal blue lines represent the average of the observed values for the four studied responses.

based on $F_{ratio\ (R/r)}$, which reflects the ratio between the mean square regression (R) and the mean square residual (r) [37].

The regression quality was measured using the coefficient of determination (R^2), while the significance of the coefficients was examined based on their *p-value* using the t-student test. The coefficient is statistically significant if the *p-value* is less than 0.05 [37]. This analysis was conducted using SAS JMP® software v.14 and Expert Design software v.12. The comparison of means was performed using the ANOVA F-test followed by Tukey's HSD test. This test compares each pair of means separately and reports on the pattern of differences between the means [38]. In the presentation of the results, the means considered statistically equivalent are attached with identical letters.

2.7.2. Optimization tools

The contour plot based on iso-response curves was employed to identify the areas of compromise leading to the desired response [39]. The optimal setting with a level of compromise was determined using the "Desirability" tool. With a percentage between 0 and 1, this tool allowed us to provide the optimal adjustment. When the components result in an undesirable reaction, the number 0 is assigned. In contrast, the maximum intended response is represented by the value 1, and each response was expressed as the mean ± standard deviation (SD). These techniques are highly helpful in determining the significance of the interactions between independent and dependent variables.

3. Results and discussion

3.1. Central composite design

The efficiency of phenolic compounds extraction, as well as the parameters that influence the antioxidant activity of *R. sphaerocarpa,* were studied by RSM. Table 2 lists the CCD parameters settings and the results of each experiment for yield, TPC, TFC, and $DPPH_{IC50}$ measurements. Every response averaged three repetitions, and the trials were conducted after randomization. It is worth noting that the recorded means for each of the four responses demonstrate a statistically significant difference (*p-value* < 0.05). Additionally, Tukey's test indicates the statistically identical means. This suggests that altering the operating circumstances significantly impacts the examined responses.

3.2. Statistical validation of the postulated model

According to the analysis of variance (Table 3), the main effect of the regression was significant for all responses since the probability of the risk significance *p-value* was less than 0.05 (0.007, 0.0044, 0.0054, and 0.0026 for yield, TPC, TFC, and $DPPH_{IC50}$, respectively). The calculation of the $F_{Ratio(R/r)}$ for the four responses showed higher values than those the $F_{(0.05;9;7)}$ at the 95% confidence level, which is equal to 3.67. Furthermore, the calculated $F_{Ratio(Lof/Pe)}$ for the four responses revealed lower values than those of $F_{(0.05;5;2)}$ at a 95% confidence level equal to 19.29. For the lack of fit test, the likelihood of a *p-value* larger than 0.05, the models are well adjusted to the observations.

Also, the coefficients of determination were equal to 0.91, 0.92, 0.91, and 0.93 for yield, TPC, TFC, and $DPPH_{IC50}$, respectively. In fact, these values demonstrated a strong correlation between experimental results and model predictions, as expressed in Fig. 1.

The obtained graphs (Fig. 1) showed that the curve of the actual values versus the predicted ones was perfectly straight for all the studied responses. Accordingly, the data approached a straight line, indicating that the anticipated data were in agreement with the experimental ones.

Table 4
Estimated regression coefficients for all responses and their level of significance *p-value*.

Terms	Coefficients	Yield		TPC		TFC		$DPPH_{IC50}$	
		Estimation	*p-value*	Estimation	*p-value*	Estimation	*p-value*	Estimation	*p-value*
Constant	b_0	18.78	<0.0001[a]	130.568	<0.0001[a]	22.76	<0.0001[a]	143.755	<0.0001[a]
Time	b_1	0.804	0.3219	2.165	0.3868	1.45	0.2010	6.277	0.0677
Solvent concentration	b_2	−1.482	0.0902	4.282	0.1107	6.91	0.0003[a]	−3.449	0.2743
Solvent-to-material ratio	b_3	5.02	0.0003[a]	13.363	0.0007[a]	2.61	0.0386[a]	−19.812	0.0003[a]
Time * Time	b_{11}	−0.12	0.9362	−26.589	0.0006[a]	3.04	0.1692	21.128	0.0071[a]
Solvent concentration * Solvent concentration	b_{22}	5.34	0.0080[a]	3.826	0.4265	3.95	0.0866	8.028	0.1960
Solvent-to-material ratio * Solvent-to-material ratio	b_{33}	−5.00	0.0110[a]	10.391	0.0556	−0.58	0.7796	−0.087	0.9881
Time * Solvent concentration	b_{12}	−0.36	0.6782	−3.19	0.2632	2.03	0.1209	−3.436	0.3256
Time * Solvent-to-material ratio	b_{13}	−0.18	0.8349	−0.51	0.8510	2.54	0.0626	7.479	0.0550
Solvent concentration * Solvent-to-material ratio	b_{23}	0.3	0.7326	−6.30	0.0472[a]	0.30	0.8045	6.059	0.1046

[a] Statistically significant at 95% confidence level.

3.3. Study of factors' effects and fitted models

The effects of all the investigated parameters, their t-student statistical values, and the observed probability (*p-value*) are depicted in Table 4. These coefficients were calculated based on the coded values of the parameters.

For the response yield, the constant b_0, the linear effects of the ethanol concentration b_3, and the quadratic effects of b_{22} and b_{33} have a significant impact since their *p-values* were lower than 0.05. The relationship between extraction yield and variables was described using the second-order polynomial equation (Eq. (3)):

$$\widehat{Y}_{Yield} = 18.78 + 5.02\, X_3 + 5.34\, X_{22}^2 - 5\, X_{33}^2 \quad (3)$$

Concerning the response TPC, and as given in Table 4, the constant b_0, the linear coefficient b_3, the quadratic term b_{11}, and the negative interaction term b_{23} were statistically significant (*p-value* < 0, 05). These results are in accordance with previously reported findings [34], who observed that the independent quadratic factors greatly impacted the recovery of phenolic compounds. The response TPC could be expressed by the following second-order polynomial equation (Eq. (4)):

$$\widehat{Y}_{TPC} = 130.56 + 13.36X_3 - 26.589X_{11}^2 - 6.30X_2X_3 \quad (4)$$

For the response TFC, the linear components b_0, b_2, and b_3 have significant coefficients. Consequently, the fitted model was represented by the following equation:

$$\widehat{Y}_{TFC} = 22.76 + 6.91X_2 + 2.61X_3 \quad (5)$$

The constant b_0, linear terms b_3, and quadratic term b_{11} were the statistically significant coefficients concerning the $DPPH_{IC50}$ response. Therefore, the fitted model was represented by the following equation (Eq. (6)):

$$\widehat{Y}_{DPPH_{IC50}} = 143.75 - 19.81X_3 + 21.12X_{11}^2 \quad (6)$$

As shown by the generated models, the four responses depend on linear terms and quadratic terms and not on interaction terms except for the negative interaction between solvent concentration and solvent/material ratio for the response TPC.

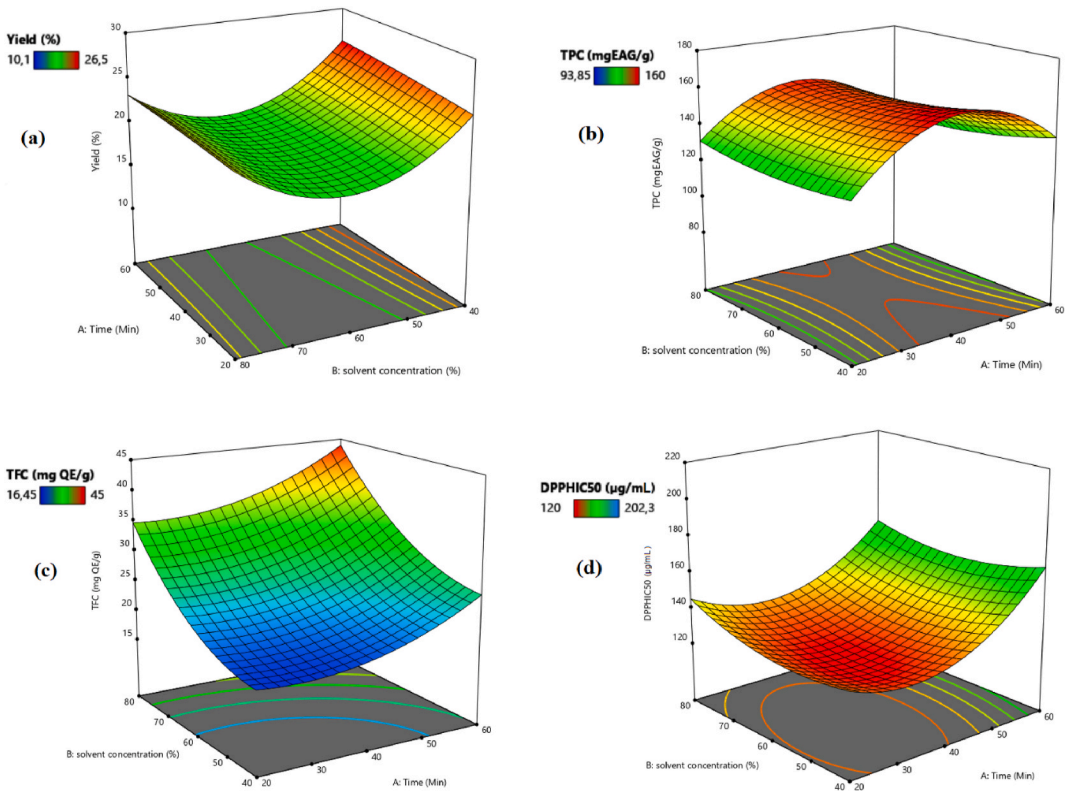

Fig. 2. Surface plots showing the optimal parameters setting leading to the best compromise zone of the four responses yield **(a)**, TPC **(b)**, TFC **(c)**, and $DPPH_{IC50}$ **(d)** obtained as a function of the two parameters time and solvent concentration by fixing the solvent-to-material ratio at 1:30.

3.4. Optimization of processing parameters

In order to judge the postulated models' quality and achieve the best value for the four responses, the contour plot based on the isoresponse curves was used. A preliminary analysis reveals that optimizing the four responses necessitates maximizing the solvent-to-material ratio. Since the isoresponse profile is a 2D representation, we must fix one of the three factors and plot the profile against the other two. We eventually decided to set this component to its optimum value in order to plot the isoresponse surfaces as a function of the two other factors.

Fig. 2 shows the four contour plots generated by fixing the third parameter (solvent-to-material ratio) into its optimal value (1:30) and representing the four responses as a function of the two parameters, extraction time and solvent concentration.

3.4.1. Optimization of the yield of extraction

As shown in the isoresponse graph (Fig. 2a), it can be seen that a yield of around 26% (red zone) can be achieved by fixing the solvent-to-material ratio to its maximum value and ensuring an extraction time between 35 and 60 min with a solvent concentration ranging from 40 to 42%. Moreover, the desirability function shows that we have a 99% chance of reaching a value of 27.6% by keeping the solvent concentration at 40%, the liquid/solid ratio at 25 mL/g, and the time factor at a maximum of 60 min (Fig. 3a). Similar results were obtained using ethanol at concentrations close to 50% to achieve a maximum value under fixed UAE conditions [15,40, 41]. Our optimized yield was higher than that of conventional extraction methods for other *retama* genus. For the species *Retama raetam*, Rejab et al. [42] have found 15.36% and 2.55% as extraction yield obtained by maceration with ethanol and hexane, respectively. Moreover, it was reported that maceration with methanol 70% gave a yield of 23.26% and 18.13% from the stems and seeds of *Retama monosperma*, respectively [43].

3.4.2. Optimization of total phenol content

As schemed in the contour plot (Fig. 2b), a value higher than 158 mg AGE/g (red zone) can be achieved by fixing the solvent-to-material ratio factor to its maximum value and by applying a time of extraction between 36 and 47 min and a solvent concentration between 40 and 45%. Besides, the desirability plot (Fig. 3b) shows that, with a 41 min extraction period, a solvent concentration of 40%, and a solvent-to-material ratio of 30 mL/g, we can generate 160 mg GAE/g DE with a desirability of 99%. Our obtained TPC is higher than the one obtained for *R. sphaerocarpa* by maceration with a mixture of methanol/water (80/20, v/v) followed by extraction with chloroform, ethyl acetate and n-butanol. In this study, the obtained TPCs were equal to 121.4 ± 0.3 GAE/g DE, 73.9 ± 0.3 GAE/g DE and 111.7 ± 0.1 GAE/g DE, respectively [43]. The same observation was made when comparing our results with obtained TPC by maceration with methanol:water (50/50 (v/v)) from *R. sphaerocarpa* seeds, which reported 125.8 ± 2.0 mg GAE/g as TPC [27]. Our findings are in agreement with those obtained by Milić et al. [44] who showed that the liquid/solid ratio had an influence on the extraction of total phenolic using UAE and reached the highest value (35.23 mg GAE/g DE) under the conditions of a liquid/solid ratio of 30%. In recent work, Ez zoubi et al. [34] reported that increasing the liquid/solid ratio up to 30 mL/g enhanced TPC recovery. Interestingly, a more excellent TPC value was achieved when the liquid-to-solid ratio was high due to the increased concentration

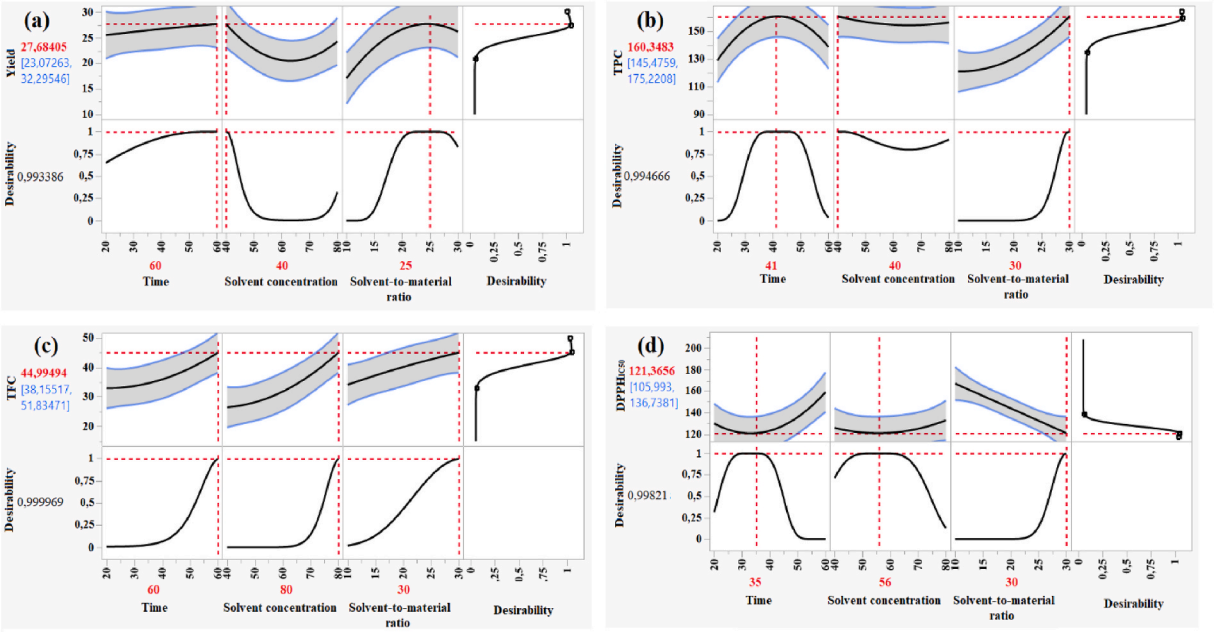

Fig. 3. Desirability plots showing the precise process setting leading to the optimal value for yield **(a)**, TPC **(b)**, TFC **(c)**, and $DPPH_{IC50}$ **(d)**, separately.

gradient. This can be explained by the fact that the surface area of the substances in contact with the solvent increased, hence enhancing the solubility of phenolic compounds in plant cells [45]. In addition to the linear effect of the solvent-to-material ratio parameter, a negative interaction was observed with the solvent concentration parameter. This means that the effect of solvent-to-material ratio was not the same in all solvent concentrations. The same findings were made for the optimization of ultrasound assisted extraction of phenolic compounds from *sparganii rhizoma*, in which a significant effect of interaction of ethanol concentration and solvent-to-material ratio [33].

Moreover, the quadratic effect of time was crucial in improving extraction efficiency (*p-value* = 0.0006). Our study showed a gradual increase in TPC recovery with an extraction time fluctuation from 20 to 40 min. Further increases beyond 40 min led to its reduction. Initially, a prolonged extraction period enhanced extraction efficiency, but afterwards, there was a clear continuous fall in the response without any impact on extraction yield. This is most likely caused by polyphenol degradation and a decrease in the solvent's polarity as previously reported [46]. This behaviour was further confirmed by other researchers, indicating that TPC recovery does not require a more extended extraction period [47]. Furthermore, previously reported data proved that a better concentration of phenolic compounds could be obtained using ultrasonic extraction while extraction time could be decreased compared to extraction by maceration [48].

3.4.3. Optimization of flavonoid content

The contour plot (Fig. 2c) showed that the predicted flavonoid content was around 40 mg EQ/g with a process set comprising a maximization of the three studied parameters. Also, the desirability function (Fig. 3c) confirms with a compromise of 99% that setting parameters at their maximum level leads to obtaining a maximum flavonoid content equal to 45 mg QE/g DE. This TFC value remains relatively high with respect to previously reported result obtained from *R. sphaerocarpa* by maceration [43], and largely high compared to that recorded through maceration of *R. raetam* [42]. According to a similar study, choosing the appropriate ratio of ethanol to water efficiently improved the extraction of valuable compounds like flavonoids [49]. However, our findings differed from those reported by Sendi et al. [2] where the optimum conditions for flavonoid recovery were a solvent-to-liquid ratio of 90 mL/g, a solvent concentration of 50%, and an extraction time of 50 min. As a result, the extraction process of flavonoids would be more feasible and efficient in potential applications that consume less solvent.

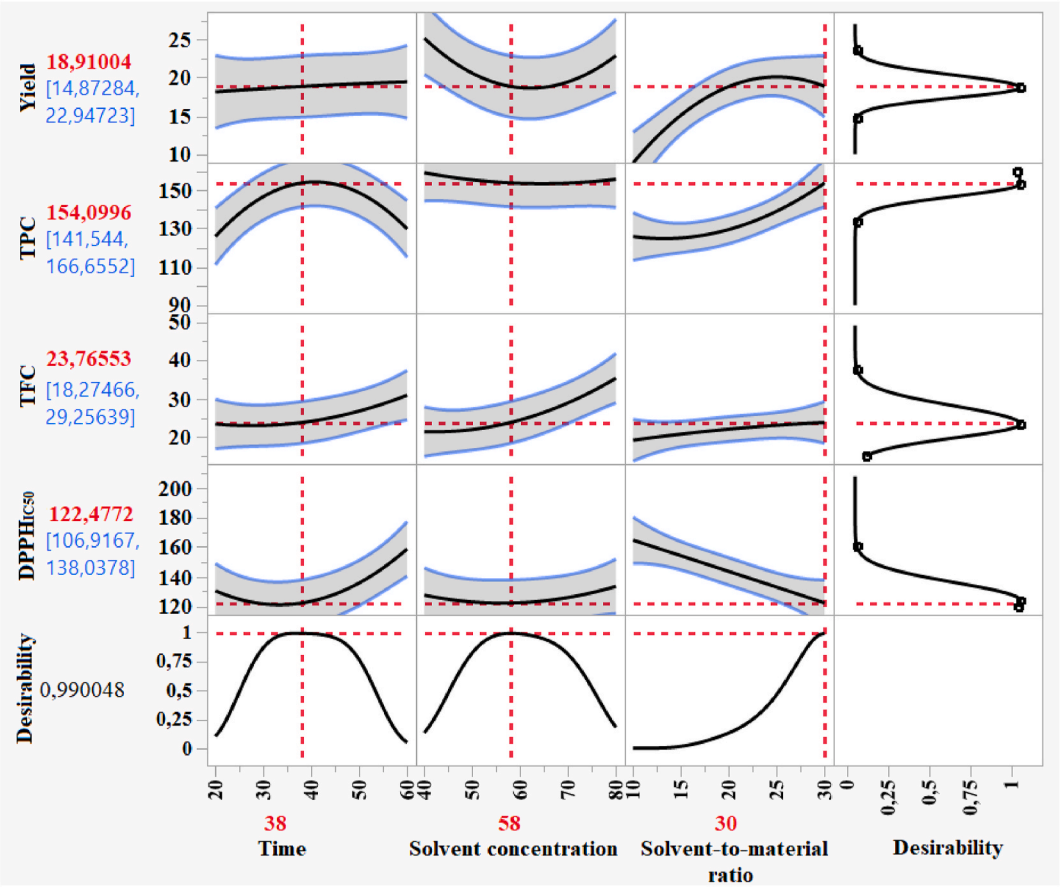

Fig. 4. Desirability plots of simultaneous optimization showing the precise values of time, solvent concentration, and solvent-to-material ratio leading to the optimal values of yield, TPC, TFC, and $DPPH_{IC50}$.

Table 5
Predicted and experimental values for the test point realized by the optimal operating conditions.

		Yield (%)		TPC (mg GAE/g)		TFC (mg QE/g)		$DPPH_{IC50}$ (μg/mL)	
Parameters	Operating setting	Predicted[a]	Experimental[b]	Predicted[a]	Experimental[b]	Predicted[a]	Experimental[b]	Predicted[a]	Experimental[b]
Extraction time	38	18.91 ± 2.38	16.62 ± 1.23	154.09 ± 7.41	160.15 ± 3.2	23.76 ± 3.24	26.91 ± 1.12	122.47 ± 9.19	128.45 ± 2.12
Solvent-to-material ratio	30								
Solvent concentration	58								

[a] The predicted value is given with the standard deviation of the response calculated from the model.
[b] The observed value is the average of three replicates with standard error.

3.4.4. Optimization of $DPPH_{IC50}$

As shown by the significance of the regression coefficients (Table 4), the solvent-to-material ratio was the most important factor impacting the DPPH radical scavenging activity, followed by the extraction time. First of all, increasing the solvent-to-material ratio toward its highest value (30 mL/g) enhanced the extraction performance. For this purpose, this factor will be fixed at its upper bound during the generation of the contour plot (Fig. 2d). This graph showed that a value of 121.7 g/mL (red zone) can be obtained by increasing the solvent-to-material ratio and ensuring a time processing between 27 and 39 min and a solvent concentration between 45 and 64%. These findings are confirmed by the desirability plot (Fig. 3d), in which the maximum value of the $DPPH_{IC50}$ response that can be achieved is equal to 121 μg/mL with a desirability of 99.1%. This value can be obtained with a time processing of 35 min, a liquid-solid ratio of 30 mL/g, and a solvent concentration of 56%. By comparing our optimized $DPPH_{IC50}$ with previous studies obtained by conventional methods, we found that it is very satisfactory compared to the results obtained by Soxhlet for the species *R. sphaerocarpa* (307.69 ± 1.33 μg/mL and 252.03 ± 3.38 μg/mL for grains and stems, respectively) [27]. In addition, Belmokhtar et al. [50] have reported a $DPPH_{IC50}$ equal to 3.15 ± 0.2 mg/mL, 1.51 ± 0.11 mg/mL, 2.88 ± 0.15 mg/mL and 3.87 ± 0.22 mg/mL for the maceration of *R. monosperma* stems in chloroform, ethyl acetate, n-butanol and methanol 70%, respectively. Although the solvent concentration had no effect on antioxidant activity in our case, it has been established that the solvent concentration has a positive effect on antiradical activity. The change in solvent polarity might justify this result as the ethanol concentration changes [51]. A recent study, Yu et al. [52] observed the same effect of ethanol concentration on antioxidant capacity of *Cimicifuga dahurica* (Turcz.) extracts. These researchers obtained an optimum IC_{50} equal to 2.48 ± 0.1780 μg/mL according to the following conditions: ethanol concentration of 56.21%, liquid/solid ratio of 14.65:1, and extraction time of 124 min. Besides, the predicted optimal extraction time for the best phenolic recovery was 41 min; this time was significantly longer than that for the best antioxidant capacity (35 min). In other words, a prolonged extraction period likely alters the extraction of phenolic chemicals, leading to a decrease in antioxidant activity. The obtained results are in agreement with the previous data by Benarfa et al. [53] who reported that excessive time might cause undesirable changes in the extracted compounds due to overexposure to ultrasonic waves.

3.4.5. Simultaneous optimization of all responses

The simultaneous optimization of all responses relies on the desirability function tool, which allows the best fit of all responses to be sought with a level of compromise. Before proceeding with the optimization of the four responses, the priority of the responses must be specified, as the maximization of one response may imply decreases in the others since the behavior of the four responses differs with regard to the studied parameters. Thus, the priority is given to the two responses, TPC and $DPPH_{IC50}$, and the optimization will be based on maximizing the first and minimizing the second.

The desirability plots in Fig. 4 indicated that optimizing all responses was possible with a desirability of 99% by ensuring an extraction time of 38 min, a solvent-to-material ratio of 30 mL/g, and a solvent concentration of 58%. The corresponding optimal response values for this setting are equal to 18.91%, a phenol content of about 154.09 mg GAE/g, a flavonoid content of approximately 23.76%, and a $DPPH_{IC50}$ of 122.47 μg/mL.

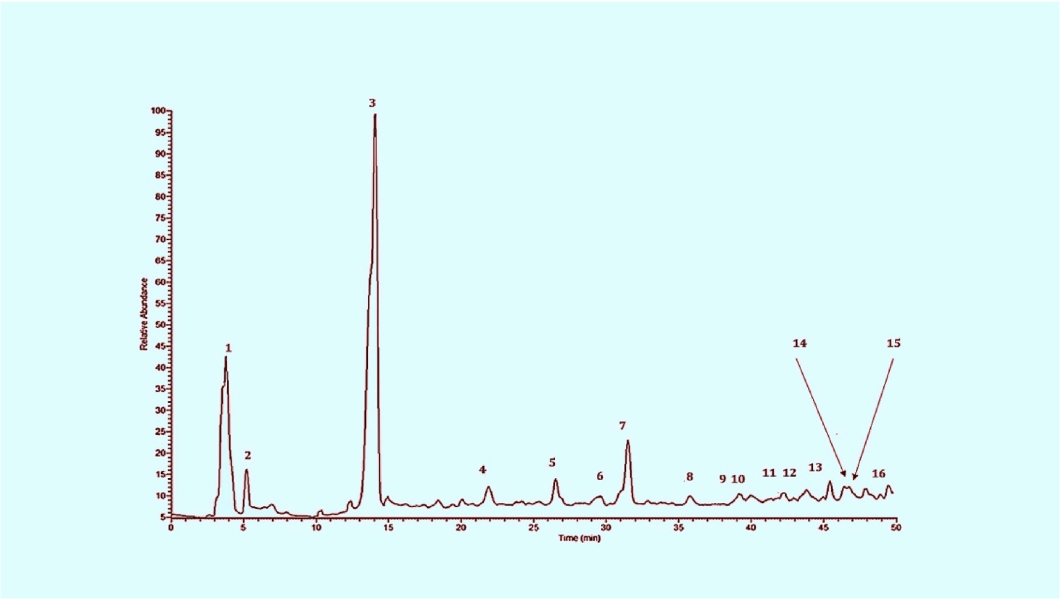

Fig. 5. LC/ESI-MS chromatographic profile recorded in the negative ion mode of *R. sphaerocarpa* extract obtained in the optimized extraction conditions.

3.4.6. Experimental validation of the optimal conditions

The accuracy of the generated models for the four responses extraction yield, TPC, TFC, and $DPPH_{IC50}$, was verified by a validation test. The test entails comparing this point's predicted results with those experimentally attained. The test coordinates were the optimal extraction conditions that gave the optimal values, producing the best ones. According to Table 5, the obtained experimental values belong to the confidence interval of the predicted values. Therefore, no noticeable difference can be observed between the experimental and predicted responses.

3.5. HPLC-ESI-MS analysis

The phenolic composition of *R. sphaerocarpa* extract was explored by liquid chromatography coupled to both PDA and MS detectors. As discussed below, fourteen compounds were identified, including two phenolic acids and twelve flavonoids. An example of the obtained chromatographic profile is indicated in Fig. 5. The obtained chromatographic and spectroscopic characteristics of each detected compound are gathered in Table 6.

3.5.1. Phenolic acids

Compound **1** (Rt = 3.75) displayed a signal at *m/z* 191 corresponding to the deprotonated molecular ion $[M-H]^-$. Other additional significant ion signals were located at *m/z* 173, 127, and 111 corresponding to $[M-H-CO-2H_2O]^-$, $[M-H-H_2O]^-$ and $[M-H-2H_2O-CO_2]^-$ ions respectively in agreement with previously reported data of quinic acid [54]. This compound is a natural antioxidant compound widely distributed in *Retama* species. Quinic acid derivatives with caffeoyl groups were reported to have higher antioxidant activities than the free acid form [55].

Compound **3** (Rt = 14.07) exhibits an $[M-H]^-$ ion signal at *m/z* 255. This compound was tentatively identified as piscidic acid on the basis of the fragment signals observed at *m/z* 193 corresponding to the $[M-H-CHO_2-OH]^-$ ion. This was also confirmed by the presence of other signals at *m/z* 165 and 119 in agreement with previously reported data of piscidic acid [56].

3.5.2. Flavonoids

Compound **5** at Rt 26.49 min showed a peak signal at *m/z* 593 corresponding to the deprotonated molecule ion $[M-H]^-$. Another signal was observed at *m/z* 431 and was associated with the loss of the *O*-hexoside moiety (−162 Da). The consecutive losses of *C*-hexosyl moiety (−90 and −120 Da) were observed in MS spectra with ion products characteristic of *C*-glycosyl flavones at *m/z* 503 and *m/z* 473, respectively [57]. Consequently, this compound was identified as vitexin-*O*-hexoside. Similarly, compounds **9** and **14** (Rt = 39.17 min and 45.39 min, respectively) were assigned to vitexin-*O*-hexoside isomers based on their UV properties characteristics of flavones with two typical absorption (one close to 320 nm and another around 260–270 nm). The proposed structures agreed with the obtained molecular ion signals observed at *m/z* 593 for both compounds. This was also reinforced by the obtained fragmentation pattern similar to apigenin-di-*O*-hexoside and especially with the characteristic fragmentations of *O*-, *C*-glycosyl flavones, with the losses of a *C*-hexosyl moiety 473 $[M-H-120]^-$ and an *O*-hexoside moiety (−162 Da) [27]. Other product ions were observed at *m/z* 431 and *m/z* 311 caused by the loss of a CO group typical of such compounds [58]. As for compound **7**, the signal at *m/z* 311 $[MH-120]^-$ showed the existence of a C-glucosyl unit based on its $[M-H]^-$ ion at *m/z* 431 pattern characteristic of a mono-C-glycoside [59]. Another vitexin derivative was detected at Rt = 42.95 (compound **12**) and was tentatively identified as vitexin-3-hydroxy-3-methylglutaroyl. Its obtained UV spectrum was comparable to those of the mentioned above vitexin isomers. The MS spectra displayed a deprotonated molecular ion at *m/z* 575 along with a product ion at *m/z* 431 and an additional loss of 144 Da, showing the 3-hydroxy-3-methylglutaroyl moiety [60].

Compound **10** (Rt = 40.27 min) was concluded to be a flavone derivative based on its UV spectral characteristics. Its MS spectra displayed a $[M-H]^-$ ion at *m/z* 593 that produced an ion at 417 $[M-H-176]^-$ as a consequence of the neutral loss of 176 Da in

Table 6
Phenolic compounds profile in *R. sphaerocarpa* obtained by optimal conditions using UHPLC-ESI-MS analysis in negative ionization mode.

Peak N°	Compound	Rt (min)	UV (nm)	$[M-H]^-$(*m/z*)	MS Product ions (*m/z*)	References	Percentage (%)
1	Quinic acid	3.75	225	191	173, 127, 111	[54,74]	3.86
2	Not identified	4.16	295	273	159	–	3.15
3	Piscidic acid	14.07	224, 275	255	193, 165, 119	[56,74]	21.02
4	Not identified	21.87	242, 373	370	239	–	1.04
5	Vitexin *O*-hexoside	26.49	232, 321	593	503, 473, 431, 311	[27,57]	11.35
6	Kaempferol di-*O*-glucoside	30.97	230, 348	609	447, 489, 285	[69,71]	4.86
7	Vitexin isomer	31.46	261, 340	431	353, 311, 283	[27]	27.60
8	Genistein *O*-hexoside	35.59	235, 264, 332	431	341, 311, 268	[65,72]	1.35
9	Vitexin *O*-hexoside	39.17	235, 266, 323	593	473, 431, 269, 311	[57]	3.82
10	Luteolin *O*-pentoside-*O*-glucoronide	40.27	233, 344	593	417, 285, 267, 241	[27]	1.73
11	Apigenin 6,8-di- *C*-hexoside	42.26	234, 262, 330	593	473, 353	[64,77,78]	3.32
12	Vitexin-3-hydroxy-3-methylglutaroyl	42.95	234, 320	575	473, 431, 311	[27]	2.13
13	Kaempferol *O*-rhamnoside	43.68	233, 269, 323	431	311, 285	[71]	3.55
14	Vitexin *O*-hexoside	45.39	233, 269, 316	593	473, 431, 311	[57]	4.17
15	Calycosin *O*-hexoside	46.74	233, 261	491	445, 283	[72,74,79]	3.86
16	Chrysin *O*-hexoside	47.87	233, 310	415	253	[73]	2.11

agreement with the structure of glucuronide acid [61]. An additional signal was observed at *m/z* 285 consistent with luteolin aglycone moiety [62]. The MS spectra of this compound also revealed a pentosyl unit loss and further water loss typical of O-hexoside units [63]. The obtained data were in agreement with a luteolin *O*-pentoside-*O*-glucuronide structure [63].

Compound **11** (Rt = 42.26 min) was determined as apigenin-6,8-di C-glycoside (vicenin 2) based on its $[M - H]^-$ at *m/z* 593. Typical fragment ion signals were observed at *m/z* 353 and 473 $[M–H–120]^-$ representing sugar cross ring cleavages in agreement with the fragmentations observed for di *C*-glycosylflavone derivatives [64]. This was also confirmed through UV spectra which were similar to those of apigenin. The MS spectra of compound **8** presented a molecular ion signal at *m/z* 431 and a fragmentation pattern signals consistent with genistein hexoside product [65]. This is consistent with previously reported data on *R. sphaerocarpa,* revealing the presence of genistein derivatives in *R. sphaerocarpa* [66]. Such derivatives were reported as the most abundant components in *Retama* species [67] and are known to exhibit high antioxidant power [68].

Compound **6** (Rt = 30.97 min) showed a signal at *m/z* 609 corresponding to the deprotonated molecular ion. Other fragment signals were observed at *m/z* 447 $[M–H–162]^-$ and *m/z* 285, resulting from the consecutive loss of two *O*-hexoside units and showing a typical fragmentations of a kaempferol aglycone moiety [69,70]. The kaempferol skeleton was confirmed based on the obtained ESI-MS spectral characteristics.

Compound **13** (Rt = 43.68 min) gave a $[M - H]^-$ ion at *m/z* 431 and its fragment signal at *m/z* 285 $[M–H–146]^-$ in agreement with a deprotonated kaempferol unit released after the neutral loss of rhamnosyl moiety (146 Da) [71]. Consequently, compound **13** was identified as kaempferol *O*-rhamnoside.

Compound **15** (Rt = 46.74 min) was tentatively identified as a methylated isoflavone derivative. Its MS spectra showed a deprotonated molecular ion $[M–H]^-$ signal at *m/z* 490. Further ion signal was observed at *m/z* 283 [M–H–162] upon fragmentation as a result of the neutral loss of the *O*-hexoside unit. Since calycosin-*O*-hexoside presents the same UV and the same fragmentation pattern [72], compound **15** was identified as calycosin *O*–hexoside.

Compound **16** (Rt = 47.87 min) was identified as chrysin *O*-hexoside based on its $[M - H]^-$ ion at *m/z* 415 and subsequent fragmentation route. The MS data of the deprotonated ion produced at *m/z* 253 suggests an *O*-glycoside substituted unit [73].

3.5.3. Relative quantitative analysis

After having studied the qualitative phytochemical composition of the obtained extract, the relative quantitative analysis of the individual identified phenolic compounds was investigated. The phenolic profile was explored using UHPLC chromatography and the obtained results are gathered in Table 6. The relative quantitation of the detected compounds has been made on the basis of the area % calculation procedure which reports the area of each peak in the chromatogram as a percentage of the total area of all peaks. This method supposes that all components respond equally in the detector and are all eluted from the column. Even if these criteria are may be not assured, the used method provides at least a suitable approximation of the relative amounts of the detected compounds.

The most prevalent classes of phenolic compounds detected in *R. sphaerocarpa* aerial parts were flavones and flavonols. Vitexin was the main compound found representing 27.60% of the extract followed by piscidic acid (21.02%) confirming the presence of phenolic acids in *Retama* species [74].

The examined sample also contained other flavonoids glycosides such as kaempferol di-*O*-glucoside (4.86%), genistein-*O*-hexoside (1.35%) and vitexin-*O*-hexoside (3.82%). Interestingly, the obtained data showed similar flavonoid content in the water: ethanol extracts both in terms of abundance and number of detected compounds compared to those previously detected in the methanol: water extracts [27]. One of the possible reasons for this similarity might be due to the solubility of *R. sphaerocarpa* leaves compounds in aqueous alcoholic solutions. Therefore, flavonoids can be best extracted by hydro-alcoholic mixture than pure alcohol or water [75]. The results obtained in the current study representing the first phytochemical investigation of *R. sphaerocarpa* leaves from Morocco are consistent with its previously reported phenolic composition [66,76]. From a qualitative point of view, the identified compounds have been previously reported in *R. sphaerocarpa* [27] with different percentages. The observed differences might be due to various variables including environmental, extraction or quantification techniques.

4. Conclusion

In this paper, a central composite design and UAE were successfully employed to optimize the extraction process of phenolic compounds from Moroccan *R. sphaerocarapa*. According to the obtained results, the simultaneous optimal extraction conditions were 38 min, 58%, and 30 mL/g for extraction time, solvent concentration, and solvent-to-material ratio, respectively. The experimental results agreed with the predicted values and provided a concept for the possible application of the obtained extracts in both scientific and industrial fields. Furthermore, the proposed UAE approach can offer an effective method for the simultaneous extraction of phenolic compounds and antiradical capacities from *R. sphaerocarpa*. Consequently, this optimized UAE method has demonstrated a potential application and provided theoretical guidance for discovering and refining potential antioxidants from *Retama* species. Moreover, the phenolic profile of *R. sphaerocarapa* proved its strong potential to serve as a source of phytochemical compounds that can be applied as bioactive agents. As a further perspective, it will be interesting to investigate other parameters influencing the extraction process, such as temperature and sonication frequency, and the mixture of solvents, which are relevant on an industrial scale and require more research and improvement.

Author contribution statement

Aafaf El Baakili, Mouhcine Fadil: Conceived and designed the experiments; Performed the experiments; Analyzed and interpreted

the data; Contributed reagents, materials, analysis tools or data; Wrote the paper.

Nour Eddine ES-SAFI: Conceived and designed the experiments; Analyzed and interpreted the data; Wrote the paper.

Data availability statement

Data included in article/supp. material/referenced in article.

Funding

This work was supported by ANPMA/UM5R/CNRST (Project number PMA2019-4).

Declaration of competing interest

The authors declare that they have no known competing financial interests or personal relationships that could have appeared to influence the work reported in this paper.

References

[1] A.G. Atanasov, S.B. Zotchev, V.M. Dirsch, C.T. Supuran, Natural products in drug discovery: advances and opportunities, Nat. Rev. Drug Discov. 20 (3) (2021) 200–216, https://doi.org/10.1038/s41573-020-00114-z.

[2] N. Sendi, N.I. Mkadmini-hammi, Khaoula Mansour Selmi, Rim Ben Sawsen Trabelsi, H. Ksouri, R. Megdiche-ksouri, Simultaneous optimization of ultrasound-assisted extraction of flavonoid compounds and antiradical activity from *Artemisia herba-Alba* using response surface methodology, Prep. Biochem. Biotechnol. 50 (9) (2020) 943–953, https://doi.org/10.1080/10826068.2020.1774778.

[3] D. Huang, Dietary antioxidants and health promotion, Antioxidants 7 (1) (2018) 9, https://doi.org/10.3390/antiox7010009.

[4] Y. Zhao, B.W.W. Grout, P. Crisp, Variations in morphology and disease susceptibility of micropropagated rhubarb (*Rheum rhaponticum*) PC49, compared to conventional plants, Plant Cell Tissue Organ Cult. 82 (2005) 357–361, https://doi.org/10.1007/S11240-005-1836-Z.

[5] G. Sharmila, V. Nikitha, S. Ilaiyarasi, K. Dhivya, V. Rajasekar, K. Manoj, K. Muthukumaran, C. Muthukumaran, Ultrasound assisted extraction of total phenolics from *Cassia auriculata* leaves and evaluation of its antioxidant activities, Ind. Crop. Prod. 84 (2016) 13–21, https://doi.org/10.1016/j.indcrop.2016.01.010.

[6] J. Zhang, C. Wen, H. Zhang, Y. Duan, H. Ma, Recent advances in the extraction of bioactive compounds with subcritical water: a review, Trends Food Sci. Technol. 95 (2019) 183–195, https://doi.org/10.1016/j.tifs.2019.11.018.

[7] A. Sridhar, M. Ponnuchamy, P. Senthil, K. Ashish, K. Dai, V.N. Vo, Techniques and modeling of polyphenol extraction from food: a review, Environ. Chem. Lett. 19 (4) (2021) 3409–3443, https://doi.org/10.1007/s10311-021-01217-8.

[8] H. Hosseini, S. Bolourian, E. Yaghoubi Hamgini, E. Ghanuni Mahababadi, Optimization of heat and ultrasound-assisted extraction of polyphenols from dried rosemary leaves using response surface methodology, J. Food Process. Preserv. 42 (11) (2018) 1–15, https://doi.org/10.1111/jfpp.13778.

[9] I.A. Mohamed, A. Fahad, A.A.R. Adisa, Optimization of ultrasound-assisted extraction of phenolic compounds and antioxidant activity from Argel (*Solenostemma argel* Hayne) leaves using response surface methodology (RSM), J. Food Sci. Technol. (2020), https://doi.org/10.1007/s13197-020-04340-6.

[10] C. Da Porto, A. Natolino, Extraction kinetic modelling of total polyphenols and total anthocyanins from saffron floral bio-residues: comparison of extraction methods, Food Chem. 258 (2018) 137–143, https://doi.org/10.1016/j.foodchem.2018.03.059.

[11] M.A. Rostagno, M. Palma, C.G. Barroso, Ultrasound-assisted extraction of soy isoflavones, J. Chromatogr. A 1012 (2003) 119–128. https://doi.org/10.1007/s13399-021-01516-8.

[12] S. Rashad, G. El-chaghaby, E.C. Lima, G. Simoes, Optimizing the ultrasonic-assisted extraction of antioxidants from *Ulva lactuca* algal biomass using factorial design, Biomass Convers. Biorefin. 13 (2021) 5681–5690. https://doi.org/10.1007/s13399-021-01516-8.

[13] L. Wang, C.L. Weller, Recent advances in extraction of nutra-ceuticals from plants, Trends Food Sci. Technol. 17 (2006) 300–312, https://doi.org/10.1016/j.tifs.2005.12.004.

[14] C.O. Perera, M.A.J. Alzahrani, Ultrasound as a pre-treatment for extraction of bioactive compounds and food safety: a review, Lwt 142 (2021), 111114, https://doi.org/10.1016/j.lwt.2021.111114.

[15] D.P. Xu, J. Zheng, Y. Zhou, Y. Li, S. Li, H. Bin Li, Ultrasound-assisted extraction of natural antioxidants from the flower of *Limonium sinuatum*: optimization and comparison with conventional methods, Food Chem. 217 (2017) 552–559, https://doi.org/10.1016/j.foodchem.2016.09.013.

[16] Ruíz-Díez Guerrouj, Beatriz Chahboune, K. Rajaa, M.H. Ramírez-Bahena, H. Abdelmoumen, M.A. Quiñones, M.M. El Idrissi, E. Velázquez, M. Fernández-Pascual, E.J. Bedmar, A. Peix, Definition of a novel symbiovar (sv. *retamae*) within *Bradyrhizobium retamae* sp. nov., nodulating Retama sphaerocarpa and Retama monosperma, Syst. Appl. Microbiol. 36 (4) (2013) 218–223, https://doi.org/10.1016/j.syapm.2013.03.001.

[17] P. Villar-Salvador, F. Valladares, S. Domínguez-Lerena, B. Ruiz-Díez, M. Fernández, F. Fernández-Pascual, A. Delgado, J.L. Peñuelas, P. Peñuelas, Functional traits related to seedling performance in the Mediterranean leguminous shrub *Retama sphaerocarpa*: insights from a provenance, fertilization, and rhizobial inoculation study, Environ. Exp. Bot. 64 (2) (2008) 145–154, https://doi.org/10.1016/j.envexpbot.2008.04.005.

[18] A. Telli, M.A. Esnault, A.O.E.H. Khelil, An ethnopharmacological survey of plants used in traditional diabetes treatment in south-eastern Algeria (Ouargla province), J. Arid Environ. 127 (2016) 82–92, https://doi.org/10.1016/j.jaridenv.2015.11.005.

[19] G. Benítez, M.R. González-Tejero, J. Molero-Mesa, Pharmaceutical ethnobotany in the western part of Granada province (southern Spain): ethnopharmacological synthesis, J. Ethnopharmacol. 129 (1) (2010) 87–105, https://doi.org/10.1016/j.jep.2010.02.016.

[20] J. Bellakhdar, La Pharmacopée Marocaine traditionnelle: Médecine arabe ancienne et savoirs populaires, Ibis Press, Country, 1997, p. 764.

[21] S. Boussahel, F. Cacciola, S. Dahamna, L. Mondello, A. Saija, F. Cimino, A. Speciale, M. Cristani, Flavonoid profile, antioxidant and antiglycation properties of *Retama sphaerocarpa* fruits extracts, Nat. Prod. Res. 32 (16) (2018) 1911–1919, https://doi.org/10.1080/14786419.2017.1356835.

[22] S. Mariem, F. Hanen, J. Inès, S. Mejdi, K. Riadh, Phenolic profile, biological activities and fraction analysis of the medicinal halophyte *Retama raetam*, South Afr. J. Bot. 94 (2014) 114–121, https://doi.org/10.1016/j.sajb.2014.06.010.

[23] K.M. Koriem, A.R. Farrag, S.A. El-Toumy, Beneficial effects of two Mediterranean medicinal plants on blood, liver, and kidney toxicity induced by formalin in rats beneficial effects of two Mediterranean medicinal plants on blood, liver, and kidney toxicity induced by formalin in rats, Biohealth. Sci. Bull. 2 (1) (2010) 8–14.

[24] N.H. González-Mauraza, A.J. León-González, J.L. Espartero, J.B. Gallego-Fernández, M. Sánchez-Hidalgo, C. Martin-Cordero, Isolation and quantification of pinitol, a bioactive cyclitol, in *Retama* spp, Nat. Prod. Commun. 11 (2016) 405–406, https://doi.org/10.1177/1934578x1601100321.

[25] L. Belayachi, C. Aceves-Luquero, N. Merghoub, Y. Bakri, S. Fernández de Mattos, S. Amzazi, P. Villalonga, *Retama monosperma* n-hexane extract induces cell cycle arrest and extrinsic pathway-dependent apoptosis in jurkat cells, BMC Compl. Alternative Med. 14 (1) (2014) 1–12, https://doi.org/10.1186/1472-6882-14-38.

[26] H. Edziri, M. Mastouri, S. Ammar, M. Matieu, G. Patrich, R. Hiar, A. Mahjoub Mohamed, S.M. Ali, L. Gutmann, M. Zine, M. Aouni, Antimicrobial, antioxidant, and antiviral activities of Retama raetam (Forssk.) Webb flowers growing in Tunisia, World J. Microbiol. Biotechnol. 24 (12) (2008) 2933–2940, https://doi.org/10.1007/s11274-008-9835-y.

[27] R. Touati, S.A.O. Santos, S.M. Rocha, K. Belhamel, A.J.D. Silvestre, Phenolic composition and biological prospecting of grains and stems of *Retama sphaerocarpa*, Ind. Crop. Prod. 95 (2017) 244–255, https://doi.org/10.1016/j.indcrop.2016.10.027.

[28] N. Ćujić, K. Šavikin, T. Janković, D. Pljevljakušić, G. Zdunić, S. Ibrić, Optimization of polyphenols extraction from dried chokeberry using maceration as traditional technique, Food Chem. 194 (2016) 135–142. https://doi.org/10.1016/j.foodchem.2015.08.008.

[29] M. Bouafia, N. Colak, F.A. Ayaz, A. Benarfa, M. Harrat, N. Gourine, M. Yousfi, The optimization of ultrasonic-assisted extraction of *Centaurea* sp. antioxidative phenolic compounds using response surface methodology, J. Appl. Res. Med. Aromat. Plants. 25 (2021) 100330. https://doi.org/10.1016/j.jarmap.2021.100330.

[30] A. Pandey, T. Belwal, K.C. Sekar, I.D. Bhatt, R.S. Rawal, Optimization of ultrasonic-assisted extraction (UAE) of phenolics and antioxidant compounds from rhizomes of *Rheum moorcroftianum* using response surface methodology (RSM), Ind. Crop. Prod. 119 (2018) 218–225, https://doi.org/10.1016/J.INDCROP.2018.04.019.

[31] J. Živković, K. Šavikin, T. Janković, N. Ćujić, N. Menković, Optimization of ultrasound-assisted extraction of polyphenolic compounds from pomegranate peel using response surface methodology, Sep. Purif. Technol. 194 (2018) 40–47, https://doi.org/10.1016/J.SEPPUR.2017.11.032.

[32] V. Nour, I. Trandafir, S. Cosmulescu, Optimization of ultrasound-assisted hydroalcoholic extraction of phenolic compounds from walnut leaves using response surface methodology, Pharm. Biol. 54 (2016) 2176–2187, https://doi.org/10.3109/13880209.2016.1150303.

[33] X. Wang, Y. Wu, G. Chen, W. Yue, Q. Liang, Q. Wu, Optimisation of ultrasound assisted extraction of phenolic compounds from *Sparganii rhizoma* with response surface methodology, Ultrason. Sonochem. 20 (2013) 846–854, https://doi.org/10.1016/J.ULTSONCH.2012.11.007.

[34] Y. Ez zoubi, M. Fadil, D. Bousta, A. El Ouali Lalami, M. Lachkar, A. Farah, Ultrasound-assisted extraction of phenolic compounds from Moroccan *Lavandula stoechas* L.: optimization using response surface methodology, J. Chem. 2021 (2021) 1–11, https://doi.org/10.1155/2021/8830902.

[35] V.L. Singleton, R. Orthofer, R.M. Lamuela-Raventós, Analysis of total phenols and other oxidation substrates and antioxidants by means of folin-ciocalteu reagent, Methods Enzymol. 299 (1999) 152–178, https://doi.org/10.1016/S0076-6879(99)99017-1.

[36] J.Y. Lin, C.Y. Tang, Determination of total phenolic and flavonoid contents in selected fruits and vegetables, as well as their stimulatory effects on mouse splenocyte proliferation, Food Chem. 101 (2007) 140–147, https://doi.org/10.1016/j.foodchem.2006.01.014.

[37] M. Fadil, S. Lebrazi, A. Aboulghazi, F.E. Guaouguaou, C. Rais, C. Slimani, N.E. Es-safi, Multi-response optimization of extraction yield, total phenols-flavonoids contents, and antioxidant activity of extracts from moroccan *Lavandula stoechas* leaves: predictive modeling using simplex-centroid design, Biocatal. Agric. Biotechnol. 43 (2022), 102430, https://doi.org/10.1016/j.bcab.2022.102430.

[38] A. Nanda, D.B.B. Mohapatra, A.P.K. Mahapatra, A.P.K. Mahapatra, A.P.K. Mahapatra, Multiple comparison test by Tukey's honestly significant difference (HSD): do the confident level control type I error, Int. J. Stat. Appl. Math. 6 (2021) 59–65, https://doi.org/10.22271/maths.2021.v6.i1a.636.

[39] M. Fadil, K. Fikri-Benbrahim, S. Rachiq, B. Ihssane, S. Lebrazi, M. Chraibi, T. Haloui, A. Farah, Combined treatment of *Thymus vulgaris* L., *Rosmarinus officinalis* L. and *Myrtus communis* L. essential oils against *Salmonella typhimurium*: optimization of antibacterial activity by mixture design methodology, Eur. J. Pharm. Biopharm. 126 (2018) 211–220, https://doi.org/10.1016/j.ejpb.2017.06.002.

[40] P. Rodsamran, R. Sothornvit, Extraction of phenolic compounds from lime peel waste using ultrasonic-assisted and microwave-assisted extractions, Food Biosci. 28 (2019) 66–73, https://doi.org/10.1016/j.fbio.2019.01.017.

[41] J. Zhou, L. Zhang, Q. Li, W. Jin, W. Chen, J. Han, Y. Zhang, Simultaneous optimization for ultrasound-assisted extraction and antioxidant activity of flavonoids from *Sophora flavescens* using response surface methodology, Molecules 24 (1) (2019) 112, https://doi.org/10.3390/molecules24010112.

[42] A. Rejab, H. Ksibi, Phenolic and flavonoid contents of some plant extracts from Tunisia southern landscape by using different extraction techniques: the case of *Retama reatam*, Med. Aromatic Plants 8 (2019) 1–6, https://doi.org/10.35248/2167-0412.19.8.337.

[43] A. Benaissa, R. Cherfia, L. Canabady-Rochelle, D. Perrin, P. Chaimbault, M. Bouhelassa, N.K. Chaouche, Antioxidant and antimicrobial potentials of *retama sphaerocarpa*, Res. J. Pharmaceut. Biol. Chem. Sci. 7 (2016) 214–221, https://doi.org/10.1080/14786419.2014.934237.

[44] A. Milić, T. Daničić, A. Tepić Horecki, Z. Šumić, D. Bursać Kovačević, P. Putnik, B. Pavlić, Maximizing contents of phytochemicals obtained from dried sour cherries by ultrasound-assisted extraction, Separations 8 (2021) 155, https://doi.org/10.3390/separations8090155.

[45] L. Yang, Y.L. Cao, J.G. Jiang, Q.S. Lin, J. Chen, L. Zhu, Response surface optimization of ultrasound-assisted flavonoids extraction from the flower of *Citrus aurantium* L. var. *amara* Engl, J. Separ. Sci. 33 (2010) 1349–1355, https://doi.org/10.1002/jssc.200900776.

[46] J. Prakash Maran, V. Sivakumar, K. Thirugnanasambandham, R. Sridhar, Optimization of microwave assisted extraction of pectin from orange peel, Carbohydr. Polym. 97 (2013) 703–709, https://doi.org/10.1016/j.carbpol.2013.05.052.

[47] L. Dumitraşcu, E. Enachi, N. Stănciuc, I. Aprodu, Optimization of ultrasound assisted extraction of phenolic compounds from cornelian cherry fruits using response surface methodology, CyTA - J. Food 17 (1) (2019) 814–823, https://doi.org/10.1080/19476337.2019.1659418.

[48] P.A. Palsikowski, L.M. Besen, E.J. Klein, C. Silva, E.A. Silva, Optimization of ultrasound-assisted extraction of bioactive compounds from *B. forficata* subsp. *Pruinosa*, Can. J. Chem. Eng. 98 (10) (2020) 2214–2226, https://doi.org/10.1002/cjce.23757.

[49] J.C. Martínez-Patiño, B. Gullón, I. Romero, E. Ruiz, M. Brnčić, J.Š. Žlabur, E. Castro, Optimization of ultrasound-assisted extraction of biomass from olive trees using response surface methodology, Ultrason. Sonochem. 51 (2019) 487–495, https://doi.org/10.1016/j.ultsonch.2018.05.031.

[50] Z. Belmokhtar, M.K. Harche, In vitro antioxidant activity of *Retama monosperma* (L.) Boiss, Nat. Prod. Res. 28 (2014) 2324–2329, https://doi.org/10.1080/14786419.2014.934237.

[51] E. Karacabey, G. Mazza, Optimisation of antioxidant activity of grape cane extracts using response surface methodology, Food Chem. 119 (1) (2010) 343–348, https://doi.org/10.1016/j.foodchem.2009.06.029.

[52] Y. Yu, C. Lv, R. Qin, M. Lv, J. Lu, Unique phenolic constituent in *Cimicifuga dahurica* (Turcz.) Maxim. through Box – behnken design and response surface methodology, J. Separ. Sci. (2019) 2550–2560, https://doi.org/10.1002/jssc.201900274.

[53] A. Benarfa, N. Gourine, S. Hachani, M. Harrat, M. Yousfi, Optimization of ultrasound-assisted extraction of antioxidative phenolic compounds from *Deverra scoparia* Coss. & Durieu (flowers) using response surface methodology, J. Food Process. Preserv. 44 (7) (2020), e14514, https://doi.org/10.1111/jfpp.14514.

[54] W.R. Corrêa, A.F. Serain, L. Aranha Netto, J.V.N. Marinho, A.C. Arena, D.F.D.S. Aquino, Â.M. Kuraoka-Oliveira, A. Jorge, L.P.T. Bernal, C.A.L. Kassuya, M. J. Salvador, Anti-inflammatory and antioxidant properties of the extract, tiliroside, and patuletin 3-O-β-D-glucopyranoside from *Pfaffia townsendii* (Amaranthaceae), evidence-based complement, Alternative Med. (2018), https://doi.org/10.1155/2018/6057579.

[55] J.Y. Choi, J.W. Lee, H. Jang, J.G. Kim, M.K. Lee, J.T. Hong, M.S. Lee, B.Y. Hwang, Quinic acid esters from *Erycibe obtusifolia* with antioxidant and tyrosinase inhibitory activities, Nat. Prod. Res. 35 (18) (2021) 3026–3032, https://doi.org/10.1080/14786419.2019.1684285.

[56] I. Gómez-López, G. Lobo-Rodrigo, M.P. Portillo, M.P. Cano, Characterization, stability, and bioaccessibility of betalain and phenolic compounds from *opuntia stricta* var. *Dillenii* fruits and products of their industrialization, Foods 10 (7) (2021) 1593, https://doi.org/10.3390/foods10071593.

[57] F. Ferreres, B.M. Silva, P.B. Andrade, R.M. Seabra, M.A. Ferreira, Approach to the study of C-glycosyl flavones by ion trap HPLC-PAD-ESI/MS/MS: application to seeds of quince (*Cydonia oblonga*), Phytochem. Anal. 14 (6) (2003) 352–359, https://doi.org/10.1002/pca.727.

[58] Y.P. Guo, H. Yang, Y.L. Wang, X.X. Chen, K. Zhang, Y.L. Wang, Y.F. Sun, J. Huang, L. Yang, J.H. Wang, Determination of flavonoids compounds of three species and different harvesting periods in *crataegi folium* based on lc-ms/ms, Molecules 26 (6) (2021) 1602, https://doi.org/10.3390/molecules26061602.

[59] A. Brito, J.E. Ramirez, C. Areche, B. Sepúlveda, M.J. Simirgiotis, HPLC-UV-MS profiles of phenolic compounds and antioxidant activity of fruits from three citrus species consumed in Northern Chile, Molecules 19 (11) (2014) 17400–17421, https://doi.org/10.3390/molecules191117400.

[60] S. Song, X. Zheng, W. Liu, R. Du, L. Bi, P. Zhang, 3-Hydroxymethylglutaryl flavonol glycosides from a Mongolian and Tibetan medicine, Oxytropis racemosa, Chem. Pharm. Bull. 58 (12) (2010) 1587–1590, https://doi.org/10.1248/cpb.58.1587.

[61] N. Fabre, I. Rustan, E. De Hoffmann, J. Quetin-Leclercq, Determination of flavone, flavonol, and flavanone aglycones by negative ion liquid chromatography electrospray ion trap mass spectrometry, J. Am. Soc. Mass Spectrom. 12 (2001) 707–715, https://doi.org/10.1016/S1044-0305(01)00226-4.

[62] S.C. Gouveia, P.C. Castilho, Artemisia annua L.: essential oil and acetone extract composition and antioxidant capacity, Ind. Crop. Prod. 45 (2013) 170–181, https://doi.org/10.1016/J.INDCROP.2012.12.022.

[63] T. Beelders, D. de Beer, M. Stander, E. Joubert, Comprehensive phenolic profiling of *Cyclopia genistoides* (L.) Vent. by LC-DAD-MS and -MS/MS reveals novel xanthone and benzophenone constituents, Molecules 19 (8) (2014) 11760–11790, https://doi.org/10.3390/molecules190811760.

[64] Z. Benayad, C. Gómez-Cordovés, N.E. Es-Safi, Characterization of flavonoid glycosides from fenugreek (*Trigonella foenum-graecum*) crude seeds by HPLC-DAD-ESI/MS analysis, Int. J. Mol. Sci. 15 (11) (2014) 20668–20685, https://doi.org/10.3390/ijms151120668.
[65] R.E. March, X.S. Miao, C.D. Metcalfe, M. Stobiecki, L. Marczak, A fragmentation study of an isoflavone glycoside, genistein-7-O-glucoside, using electrospray quadrupole time-of-flight mass spectrometry at high mass resolution, Int. J. Mass Spectrom. 232 (2) (2004) 171–183, https://doi.org/10.1016/j.ijms.2004.01.001.
[66] S. Louaar, S. Akkal, H. Laouer, D. Guilet, Flavonoids of *Retama sphaerocarpa* leaves and their antimicrobial activities, Chem. Nat. Compd. 43 (2007) 616–617, https://doi.org/10.1007/s10600-007-0207-x.
[67] M. López-Lázaro, C. Martín-Cordero, F. Cortés, J. Piñero, M.J. Ayuso, Cytotoxic activity of flavonoids and extracts from *Retama sphaerocarpa Boissier*, Zeitschrift Fur Naturforsch. - Sect. C J. Biosci. 55 (1-2) (2000) 40–43, https://doi.org/10.1515/znc-2000-1-209.
[68] A. Kładna, I. Berczyński Paweł and Kruk, T. Piechowska, H.Y. Aboul-Enein, Studies on the antioxidant properties of some phytoestrogens, Luminescence (2016) 1201–1206, https://doi.org/10.1002/bio.3091.
[69] L.N. Francescato, S.L. Debenedetti, T.G. Schwanz, V.L. Bassani, A.T. Henriques, Identification of phenolic compounds in *Equisetum giganteum* by LC-ESI-MS/MS and a new approach to total flavonoid quantification, Talanta 105 (2013) 192–203, https://doi.org/10.1016/j.talanta.2012.11.072.
[70] E.J. Oliveira, D.G. Watson, In vitro glucuronidation of kaempferol and quercetin by human UGT-1A9 microsomes, FEBS Lett. 471 (1) (2000) 1–6, https://doi.org/10.1016/S0014-5793(00)01355-7.
[71] L. Barros, E. Pereira, R.C. Calhelha, M. Dueñas, A.M. Carvalho, C. Santos-Buelga, I.C.F.R. Ferreira, Bioactivity and chemical characterization in hydrophilic and lipophilic compounds of *Chenopodium ambrosioides* L, J. Funct.Foods 5 (2013) 1732–1740, https://doi.org/10.1016/j.jff.2013.07.019.
[72] M. Ye, W.Z. Yang, K. Di Liu, X. Qiao, B.J. Li, J. Cheng, J. Feng, D.A. Guo, Y.Y. Zhao, Characterization of flavonoids in *Millettia nitida* var. *hirsutissima* by HPLC/DAD/ESI-MSn, J. Pharm. Anal. 2 (1) (2012) 35–42, https://doi.org/10.1016/j.jpha.2011.09.009.
[73] C. Bastos, L. Barros, M. Dueñas, R.C. Calhelha, M.J.R.P. Queiroz, C. Santos-Buelga, I.C. Ferreira, Chemical characterisation and bioactive properties of *Prunus avium* L.: the widely studied fruits and the unexplored stems, Food Chem. 173 (2015) 1045–1053, https://doi.org/10.1016/j.foodchem.2014.10.145.
[74] M. Saada, H. Falleh, M.D. Catarino, S.M. Cardoso, R. Ksouri, Plant growth modulates metabolites and biological activities in *Retama raetam* (forssk.) webb, Molecules 23 (9) (2018) 2177, https://doi.org/10.3390/molecules23092177.
[75] Q.D. Do, A.E. Angkawijaya, P.L. Tran-Nguyen, L.H. Huynh, F.E. Soetaredjo, S. Ismadji, Y.H. Ju, Effect of extraction solvent on total phenol content, total flavonoid content, and antioxidant activity of *Limnophila aromatica*, J. Food Drug Anal. 22 (3) (2014) 296–302, https://doi.org/10.1016/j.jfda.2013.11.001.
[76] S. Louaar, S. Akkal, A. Bousetla, K. Medjroubi, L. Djarri, E. Seguin, Phytochemical study of *Retama sphaerocarpa*, Chem. Nat. Compd. 41 (2005) 107–108, https://doi.org/10.1007/s10600-005-0091-1.
[77] L. Hu, Z. Liang, Y. Wang, G. Wei, Y.C. Huang, Identification of C-glycosyl flavones and O-glycosyl flavones in five Dendrobium species by high-performance liquid chromatography coupled with electrospray ionization multi-stage tandem MS, Rapid Commun. Mass Spectrom. 36 (2022), e9158, https://doi.org/10.1002/RCM.9158.
[78] J.C.M. Barreira, E. Pereira, M. Dueñas, A.M. Carvalho, C. Santos-Buelga, I.C.F.R. Ferreira, *Bryonia dioica, Tamus communis* and *Lonicera periclymenum* fruits: characterization in phenolic compounds and incorporation of their extracts in hydrogel formulations for topical application, Ind. Crop. Prod. 49 (2013) 169–176, https://doi.org/10.1016/J.INDCROP.2013.04.057.
[79] X. Qiao, W. Song, S. Ji, Y. jiao Li, Y. Wang, R. Li, R. An, D. an Guo, M. Ye, Separation and detection of minor constituents in herbal medicines using a combination of heart-cutting and comprehensive two-dimensional liquid chromatography, J. Chromatogr., A 1362 (2014) 157–167, https://doi.org/10.1016/J.CHROMA.2014.08.038.